

Spin Diffusion in Trapped Gases: Anisotropy in Dipole and Quadrupole Modes.

W. J. Mullin¹ and R. J. Ragan²

¹*Physics Department, Hasbrouck Laboratory,*

University of Massachusetts, Amherst, MA 01003 and

²*Physics Department, University of Wisconsin at Lacrosse, La Crosse, WI 54601*

(Dated: March 23, 2022)

Abstract

Recent experiments in a mixture of two hyperfine states of trapped Bose gases show behavior analogous to a spin-1/2 system, including transverse spin waves and other familiar Leggett-Rice-type effects. We have derived the kinetic equations applicable to these systems, including the spin dependence of interparticle interactions in the collision integral, and have solved for spin-wave frequencies and longitudinal and transverse diffusion constants in the Boltzmann limit. We find that, while the transverse and longitudinal collision times for trapped Fermi gases are identical, the Bose gas shows unusual diffusion anisotropy in both dipole and quadrupole modes. Moreover, the lack of spin isotropy in the interactions leads to the non-conservation of transverse spin, which in turn has novel effects on the hydrodynamic modes.

PACS numbers: 03.75.Mn, 05.30.Jp, 05.60.Gg, 51.10.+y, 67.20.+k.

I. INTRODUCTION

In JILA experiments,[1],[2] a mixture of two hyperfine states was found to segregate by species. The theoretical explanation[3]-[8] for this behavior is based on the two states playing the role of a pseudo-spin-1/2 system, having transverse spin waves. The theory of these new effects is based on old ideas of the transport properties of polarized homogeneous quantum gases of real spins, such as ^3He gas and solutions of ^3He in liquid ^4He , [9],[10] transcribed to the trapped gas pseudo-spin case.

Besides spin waves, the theory for homogeneous polarized fermions or bosons led to the prediction of anisotropic spin diffusion in the degenerate state.[9],[10],[11] When a spin nonuniformity is longitudinal, that is, with a variation in the magnitude of the magnetization, the spin diffusion coefficient is D_{\parallel} . On the other hand, in a spin-echo experiment, the magnitude of the magnetization is uniform but it varies spatially in direction. The corresponding diffusion coefficient, D_{\perp} is less than D_{\parallel} when the system is polarized and degenerate. Experimentally this feature has been seen, but was not always in reasonable accord with theory.[9] Further, Fomin[12] has suggested the effect should not exist. However, a recent experiment[9] has overcome several possible experimental objections and finds good agreement with theory. Moreover recent papers[13],[14] have presented theoretical analyses that question the validity of Fomin's approach.

Thus it seems useful to see whether a similar difference between longitudinal and transverse diffusion in trapped gases might provide an alternative testing ground for this question. However, what we show here is that the physical possibility of having differing interaction parameters between up-up, down-down, and up-down states (interaction anisotropy) provides a new physical basis for anisotropic spin diffusion for bosons even in the Boltzmann limit.[16] For longitudinal diffusion in the Boltzmann limit only up-down scattering contributes. However, in the transverse case, two spins at differing angles approach one another, and the scattering can be analyzed as being a superposition of, say, up-up and up-down scattering. In the fermion s-wave case, the up-up part gives no contribution, and, in the Boltzmann limit, the diffusion coefficients are identical. In that case one must go to the degenerate limit to see the anisotropy, which then is expected to arise because the density of scattering states differs in longitudinal and transverse cases.[10] On the other hand, for bosons, for which both the up-up and down-down scattering rates do contribute, we find

an anisotropy even in the Boltzmann limit, but only if the various scattering lengths differ. We have here the interesting effect that, although both gases obey Boltzmann statistics, there is a macroscopic difference between fermion and boson behavior because of quantum statistical effects in the two-particle scattering. Moreover in the Bose case a new element enters: the interaction now introduces a spin-spin relaxation mechanism (a T_2 process) so that transverse magnetization is no longer conserved.[7] For very small relaxation times τ , the hydrodynamic relaxation rate is no longer linear in τ ; now it diverges. For fermions it remains well behaved.

Below we first use the moments method to compute the spectra of the lowest-lying longitudinal and transverse modes. However, with that method we obtain a transverse decay rate γ_\perp that diverges as τ approaches zero, in contrast to the usual diffusive behavior where $\gamma_\perp \propto \tau$. In this case it is necessary to solve the *local* hydrodynamic equations to find the correct behavior, in which the hydrodynamic solutions are localized at the low-density regions at the edges of the cloud where the collision time is longer. The result is a much smaller decay rate than that obtained with the moments method.

In helium the dipole modes were detected experimentally, but in the trapped gases it was more convenient to look at the quadrupole modes.[1], [2] Thus we calculate both here. We have previously reported results on the dipolar modes.[15]

In our previous work, Ref. 10, we derived an analog of the Landau-Silin equation for a 2×2 density operator \hat{n}_p (here acting in the pseudo-spin space), with effective mean-field single particle energy matrix $\hat{\epsilon}_p$. We can write the density and single-particle energy in a Pauli representation as $\hat{n}_p = \frac{1}{2} (f_p \hat{I} + \mathbf{m}_p \cdot \hat{\sigma})$ and $\hat{\epsilon}_p = (e_p \hat{I} + \mathbf{h}_p \cdot \hat{\sigma})$ where $\hat{\sigma}$ is a Pauli matrix, $\frac{1}{2}(f_p \pm m_{pz})$ give the diagonal components of the density $n_{pi} = n_{pii}$, and \mathbf{m}_p represents the polarization, which in equilibrium is along the axis $\hat{\mathbf{z}}$. We find the following approximate equation for \mathbf{m}_p :

$$\frac{\partial \mathbf{m}_p}{\partial t} - \frac{2}{\hbar} \mathbf{h} \times \mathbf{m}_p + \sum_i \left[\frac{p_i}{m} \frac{\partial \mathbf{m}_p}{\partial r_i} - \frac{\partial U}{\partial r_i} \frac{\partial \mathbf{m}_p}{\partial p_i} \right] = \text{Tr} \{ \hat{\sigma} \hat{I}_p \} \quad (1)$$

with $m_{pz}(\mathbf{r}) = n_{p1} - n_{p2}$ and $n_{p12}(\mathbf{r}) = n_{p21}^* = \frac{1}{2} m_{p-}(\mathbf{r}) = \frac{1}{2} (m_{px} - i m_{py})$. The 2×2 collision integral is \hat{I}_p . The effective mean magnetic field is

$$\mathbf{h} = \frac{\hbar \Omega_0}{2} \hat{\mathbf{z}} + \eta \frac{t_{12}}{2} \mathbf{M} \quad (2)$$

where

$$\hbar \Omega_0 = V_1 - V_2 + [(t_{11} - t_{12}) n_1 - (t_{22} - t_{12}) n_2] (1 + \eta). \quad (3)$$

In these η is 1 (-1) for bosons (fermions); $\mathbf{M}(\mathbf{r}) = \int d\mathbf{p}/h^3 \mathbf{m}_p(\mathbf{r})$; $n_i(\mathbf{r}) = \int d\mathbf{p}/h^3 n_p(\mathbf{r})$; V_i is the external field for species i ; $U = \frac{1}{2}(V_1 + V_2)$; and $M_z = n_1 - n_2$. The t 's can be evaluated in terms of the measured scattering lengths $a_{\alpha\beta}$ by using $t_{\alpha\beta} = 4\pi\hbar a_{\alpha\beta}/m$.

The equilibrium solution in the Boltzmann limit is $m_p^{(0)} = \mathcal{M}(\beta\hbar\bar{\omega})^3 \exp[-\beta(p^2/2m + U)]$ where N is the total number of particles, N_i is the number of species i , $\mathcal{M} = N_1 - N_2$ is the total magnetization, and $\bar{\omega} \equiv (\omega_x\omega_y\omega_z)^{1/3}$.

We have derived the collision integral for the Boltzmann case when the various interaction parameters differ. Our expression agrees with the same quantity derived in Refs. 7 and 8, and reduces properly to previous results if all the t 's are taken equal.[10],[17] We find

$$\begin{aligned}
(\sigma|\hat{L}_p|\sigma') &= \frac{\pi}{\hbar} \int d\mathbf{p}_1 d\mathbf{p}_2 d\mathbf{p}_3 \delta(\mathbf{p}_1 + \mathbf{p}_2 - \mathbf{p}_3 - \mathbf{p}_4) \delta(\epsilon_{\mathbf{p}_1} + \epsilon_{\mathbf{p}_{21}} - \epsilon_{\mathbf{p}_{31}} - \epsilon_{\mathbf{p}_4}) \\
&\quad \sum_{\sigma_2} \left\{ -t_{\sigma\sigma_2}^2 [(n_{\mathbf{p}_1})_{\sigma\sigma'} (n_{\mathbf{p}_2})_{\sigma_2\sigma_2} + \eta(n_{\mathbf{p}_2})_{\sigma\sigma_2} (n_{\mathbf{p}_1})_{\sigma_2\sigma'}] \right. \\
&\quad - t_{\sigma'\sigma_2}^2 [(n_{\mathbf{p}_1})_{\sigma\sigma'} (n_{\mathbf{p}_2})_{\sigma_2\sigma_2} + \eta(n_{\mathbf{p}_1})_{\sigma\sigma_2} (n_{\mathbf{p}_2})_{\sigma_2\sigma'}] \\
&\quad \left. + 2t_{\sigma\sigma_2} t_{\sigma'\sigma_2} [(n_{\mathbf{p}_3})_{\sigma\sigma'} (n_{\mathbf{p}_4})_{\sigma_2\sigma_2} + \eta(n_{\mathbf{p}_3})_{\sigma\sigma_2} (n_{\mathbf{p}_4})_{\sigma_2\sigma'}] \right\} \quad (4)
\end{aligned}$$

We will linearize the kinetic equation for \mathbf{m}_p around the global equilibrium value $m_p^{(0)}\hat{\mathbf{z}}$ and use a moment approach to compute the spin wave and diffusive damping just as done previously.[5],[7] The linearized longitudinal and transverse equations are

$$\frac{\partial \delta m_{pz}}{\partial t} + \sum_i \left[\frac{p_i}{m} \frac{\partial \delta m_{pz}}{\partial r_i} - \frac{\partial U}{\partial r_i} \frac{\partial \delta m_{pz}}{\partial p_i} \right] = \sum_{\sigma} \sigma (\sigma|\hat{L}_p|\sigma) \quad (5)$$

and

$$\begin{aligned}
&\frac{\partial \delta m_{p+}}{\partial t} + i \frac{\eta t_{12}}{\hbar} (m_p^{(0)} \delta M_+ - M_0 \delta m_{p+}) - i \Omega_0 \delta m_{p+} \\
&+ \sum_i \left[\frac{p_i}{m} \frac{\partial \delta m_{p+}}{\partial r_i} - \frac{\partial U}{\partial r_i} \frac{\partial \delta m_{p+}}{\partial p_i} \right] = 2(2|\hat{L}_p|1). \quad (6)
\end{aligned}$$

where \hat{L}_p is the linearized form of \hat{L}_p .

In the next section we compute results for the monopole and dipole modes. Experiments have detected the quadrupole modes which we study in the third section.

II. DIPOLE MODES

A. a. Longitudinal dipole.

We use a variational function of the form

$$\delta m_{pz} = (a_0 + a_1 \tilde{z} + a_2 \tilde{p}_z) m_p^{(0)} \quad (7)$$

with \tilde{x} being position in units of $(\beta m)^{-1/2} \omega_i^{-1}$ and \tilde{p}_i momentum in units of $(m/\beta)^{1/2}$. We take the 1, z , and p_z moments of the kinetic equation in both the longitudinal and transverse cases. The results for the longitudinal case, if we assume a time dependence of $\exp(i\omega t)$ for a_1 and a_2 , are

$$da_0/dt = 0 \quad (8)$$

$$i\omega a_1 - \omega_z a_2 = 0 \quad (9)$$

$$i\omega a_2 + \omega_z a_1 = -\gamma_{\parallel} a_2 \quad (10)$$

with

$$\gamma_{\parallel} = \frac{4\gamma_0}{3} \quad (11)$$

and

$$\gamma_0 = \frac{\pi \beta m^3 \bar{\omega}^3 t_{12}^2 N}{h^4} \quad (12)$$

coming from integrating the collision integral. Eq. (8) indicates that the monopole mode does not decay in the longitudinal case, which is consistent with the conservation of magnetization. The effective external field Ω_0 does not enter into the longitudinal modes. The second line is the magnetization equation of continuity. The relaxation rate γ_{\parallel} agrees with that derived in Ref. 5. To find the modes one simply solves a quadratic equation. The dipole spectrum is plotted in Fig. 1 as a function of $\tau_{\parallel} \equiv 1/\gamma_{\parallel}$, the *spatially averaged* collision time. In the small $\omega_z \tau_{\parallel}$ limit, one finds

$$\omega = i\omega_z^2 \tau_{\parallel}, \quad (13)$$

which has the form of the lowest-order solution of a diffusion equation in a harmonic potential. The other solution for small $\omega_z \tau_{\parallel}$ is the high frequency mode

$$\omega = i \frac{1}{\tau_{\parallel}}. \quad (14)$$

The first of these solutions, the diffusive mode, is mainly a z mode while the second mainly a momentum dipole. For large $\omega_z \tau_{\parallel}$ the solutions have roughly equal magnitudes of a_1 and a_2 with frequencies

$$\omega = \pm \omega_z + \frac{i}{\tau_{\parallel}}. \quad (15)$$

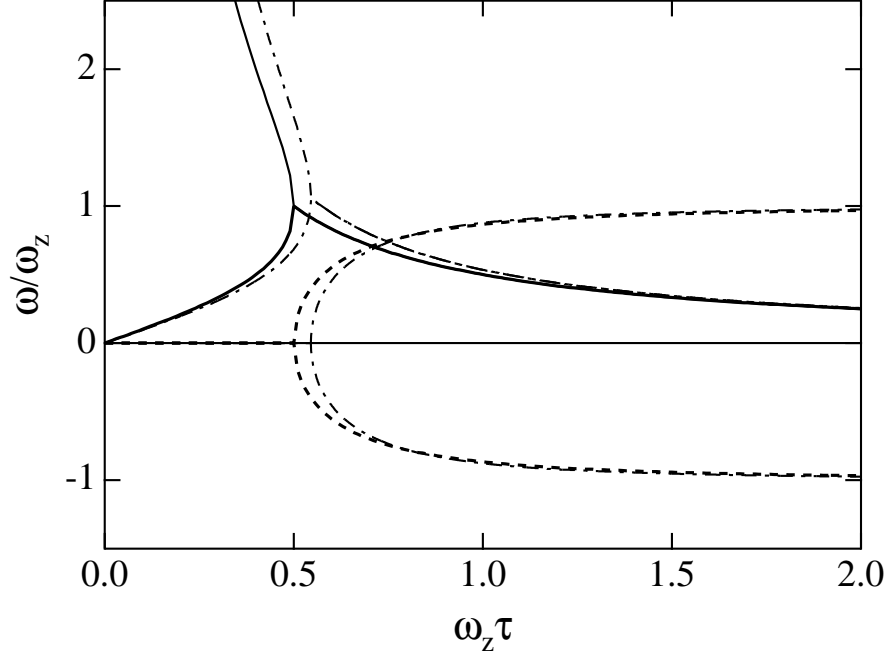


FIG. 1: Real (dashed) and imaginary (solid) components of longitudinal dipole spin wave modes versus average relaxation time τ_{\parallel} . Note the linear dependence of $\text{Im}(\omega)$ for small τ_{\parallel} characteristic of diffusive behavior. The dash-dotted lines represent the results of a numerical calculation to be discussed below.

B. b. Transverse dipole.

We again use the form of Eq. (7). We also assume that the effective external field Ω_0 is quadratic in position, that is, the part $V_1 - V_2$ dominates the density dependent part in Eq. (3). We write

$$\Omega_0 = \Delta_{\perp}(\tilde{x}^2 + \tilde{y}^2) + \Delta_z \tilde{z}^2.$$

Taking 1, z , and p_z moments of Eq. (6) yields the results

$$da_0/dt - i\omega_0 a_0 = -\gamma_T a_0 \quad (16)$$

$$i(\omega - \omega_0 - \omega_{\parallel}) a_1 - \omega_z a_2 = -\frac{1}{2} \gamma_T a_1 \quad (17)$$

$$i(\omega - \omega_M - \omega_0) a_2 + \omega_z a_1 = -\gamma_{\perp} a_2 \quad (18)$$

where ω_0 and ω_{\parallel} are parts of the effective field:

$$\omega_0 = 2\Delta_{\perp} + \Delta_z$$

$$\omega_{\parallel} = 2\Delta_z$$

$$\gamma_T = \gamma_0(1 + \eta) \sum_{\sigma} \left(\frac{t_{\sigma\sigma} - t_{12}}{t_{12}} \right)^2 f_{\sigma}$$

with $f_{\sigma} = N_{\sigma}/N$, and

$$\gamma_{\perp} = \gamma_{\parallel} \left[\frac{7R - 3S}{8t_{12}^2} \right] \quad (19)$$

with $R = (1 + \eta) \sum_{\sigma} t_{\sigma\sigma}^2 f_{\sigma} + (1 - \eta) t_{12}^2$ and $S = 2t_{12}[(1 + \eta) \sum_{\sigma} t_{\sigma\sigma} f_{\sigma} - \eta t_{12}]$, and the mean-field frequency is

$$\omega_M = \eta \frac{t_{12} \mathcal{M}}{\hbar} \left(\frac{\beta \hbar \bar{\omega}}{\sqrt{2} \lambda} \right)^3 \quad (20)$$

where λ is the thermal wavelength. Since ω_0 occurs in each equation we can remove it by including a time dependence $e^{i\omega_0 t}$ in each a_i ; that is, we go into the frame rotating at ω_0 . We assume this is done and all frequencies and will neglect this constant part.

Comments:

1) If the interactions parameters t_{ij} are all equal, we have $\gamma_T = 0$, $R = S = 2t^2$ so that $\gamma_{\perp} = \gamma_{\parallel}$. Eqs. (16)-(18) then reduce to those of Ref. 5 and the longitudinal and transverse relaxation rates are the same, which agrees with the standard result for a homogeneous real spin system in the Boltzmann limit.

2) For fermions, we have $\eta = -1$, so that, even if the t 's are *not* equal, $\gamma_T = 0$ and $\gamma_{\perp} = \gamma_{\parallel}$. In the s -wave limit only up-down scattering occurs for fermions and there can be no anisotropy in the Boltzmann limit.

3) For bosons with unequal t 's, the spatial averaged transverse relaxation rate is not generally the same as the longitudinal. Moreover, we have a T_2 -type relaxation rate for a_0 and in the equation of continuity (17). The interaction anisotropy behaves something like a dipole-dipole interaction allowing relaxation of the transverse spin, an effect noted previously in Ref. 7.

If, for now, we take $\gamma_T = 0$, then the lowest mode in the hydrodynamic limit ($\omega_z \tau_{\parallel} \ll 1$) takes the form

$$\omega = \omega_{\parallel} + \frac{\omega_z^2(i - \bar{\omega}_M \tau_{\perp})\tau_{\perp}}{[1 + (\bar{\omega}_M \tau_{\perp})^2]}. \quad (21)$$

where $\tau_{\perp} \equiv 1/\gamma_{\perp}$, and $\bar{\omega}_M = \omega_M - \omega_{\parallel}$. The so-called “spin-rotation parameter” from Leggett-Rice systems is $\mu = \bar{\omega}_M \tau_{\perp}/\mathcal{M}$. The form of Eq. (21) is the hydrodynamic frequency as modified by spin rotation. [9],[10],[17]. The first term in the fraction is the effective diffusion frequency while the second is the dipole-mode pseudo-spin-wave frequency. This diffusive mode is now shifted by the effective external field, ω_{\parallel} . This mode is the z dipole mode; whereas the p -mode is found to be

$$\omega = \omega_M + \frac{i}{\tau_{\perp}} \quad (22)$$

which again diverges as τ_{\perp} gets small.

For large $\omega_z \tau_{\perp}$ we find the pair of frequencies

$$\omega = \pm \omega_z + \frac{1}{2}(\omega_M + \omega_{\parallel}) + \frac{i}{2\tau_{\perp}}. \quad (23)$$

The effect of non-zero γ_T is to allow a T_2 relaxation of the transverse spins. The results are shown in Fig. 2, where we have set $1/\tau_{\perp} = \gamma_{\parallel}$, $\gamma_T = 0.02/\tau_{\perp}$, and $\bar{\omega}_M = \omega_z$. In the small τ_{\perp} limit, one no longer has the hydrodynamic decay rate approaching zero, but instead it diverges at the origin because $\text{Im}(\bar{\omega}) \approx (\omega_z^2 \tau_{\perp} + \gamma_T)$, and $\gamma_T \sim 1/\tau_{\perp}$. However, although suitable for finite $\omega\tau$, the moments method is inadequate in the hydrodynamic limit. It fails because the simple forms assumed for spatial dependence cannot adjust to the spatially dependent relaxation rates. One must solve local equations numerically for the spatial behavior.

To obtain the hydrodynamic equations we expand the momentum distribution in terms of Hermite polynomials

$$\delta m_{pz} = e^{-\beta p^2/2m} \sum_{k=0} c_k(z, t) H_k(p) \quad (24)$$

Substituting this into the kinetic equations, neglecting terms in ω_{\parallel} , integrating over the momentum, and keeping terms lowest order in τ_{\perp} gives, in the transverse case,

$$\partial_t \delta M_+ + \partial_z J_+ = -\gamma_T(z) \delta M_+ \quad (25)$$

$$\partial_t J_+ + \frac{kT}{m} \partial_z \delta M_+ + \omega_z^2 z \delta M_+ + i\omega_M(z) J_+ \approx -\gamma_{\perp}(z) J_+ \quad (26)$$

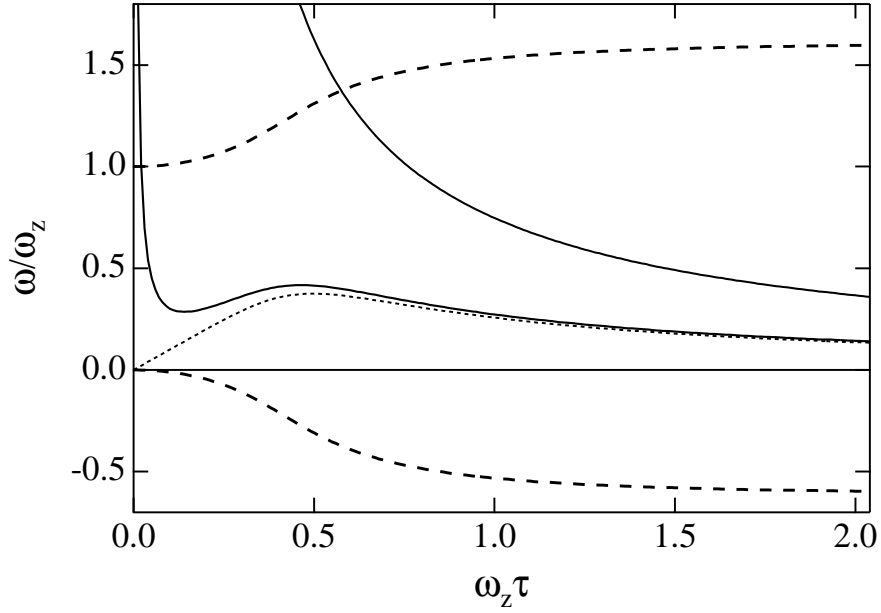


FIG. 2: Real (dashed) and imaginary (solid) components of transverse dipole spin wave modes versus average relaxation time τ_{\perp} when the transverse spin is not conserved. The dotted line shows the lower imaginary mode when the transverse decay rate $\gamma_T = 0$. In this plot $\omega_M/\omega_z = 1$, $\omega_{\parallel} = 0$. The linear behavior of $\text{Im}(\omega)$ for small τ_{\perp} characteristic of diffusive behavior is destroyed and replaced by a divergence within the moments method used here.

where $\delta M_{+}(z, t) = c_0(z, t)$ is the nonequilibrium magnetization density, $J(z, t) = \int d\mathbf{p}/h^3 (p/m) \delta m_{pz} = c_1(z, t)$ is the spin current, and $\gamma_{\perp}(z) = \gamma_{\perp}(0) \exp(-\beta m \omega_z^2 z^2/2)$. Analogous equations hold in the longitudinal case. On the RHS of Eq. (26) the $k = 1$ momentum distribution has been treated as an eigenfunction of the linearized collision integral. This is justified by a numerical calculation of the matrix elements of the collision integral, which gives

$$\begin{aligned} L_{\perp}[H_1(p)] &= -\gamma_{\perp}(0)(1.000H_1(p) + 0.123H_3(p) \\ &\quad - 0.00094H_5(p) + \dots) \approx -\gamma_{\perp}(0)H_1(p) \end{aligned} \quad (27)$$

The eigenvalues of the hydrodynamic equations have been calculated numerically for the dipole mode with boundary conditions $\delta M(0) = 0$, $J(0) = 1$, and $J(\infty) = 0$, and the monopole mode with boundary conditions $\delta M(0) = 1$, $J(0) = 0$, and $J(\infty) = 0$. For the longitudinal and isotropic transverse cases this leads to only small corrections to the $\tau \rightarrow 0$ part of the spectra obtained by the moments method as shown in Fig. 1.

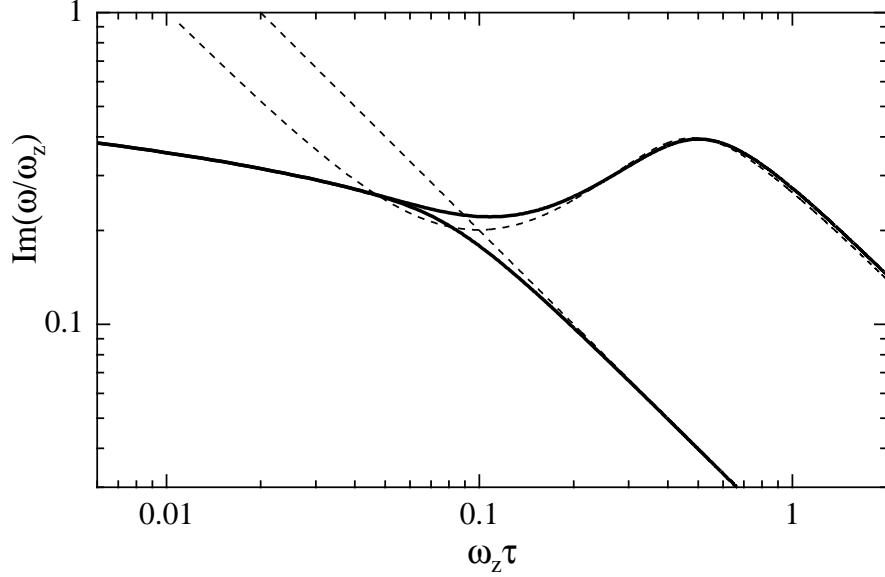


FIG. 3: Imaginary part of the spin-wave spectrum vs. $\omega_z \tau_\perp$ for the monopole and dipole modes with $\omega_M = \omega_z$, $\gamma_T = 0.02\gamma_\perp$, $\omega_\parallel = 0$, and $\gamma_\perp \approx \gamma_\parallel$ for both the moments method (dashed) and hydrodynamic calculations (solid).

However, for $\gamma_T > 0$ the hydrodynamic spectrum differs qualitatively from that of the moments method calculation. As $\tau_\perp \rightarrow 0$ the hydrodynamic dipole and monopole modes do not decay at a rate $\sim 1/\tau_\perp$, but instead decay at a slower rate. For $\omega_z \tau_\perp \ll \alpha = \gamma_T \tau_\perp$, the hydrodynamic equations can be Taylor expanded about the center of an effective complex potential, giving a decay rate $\omega_z \sqrt{2\alpha \log(\sqrt{\alpha}/\omega_z \tau_\perp)}$ (See Fig. 3.) At small enough $\omega_z \tau_\perp$ the T_2 decay of the magnetization at the center of the trap causes the monopole and dipole modes to coalesce into spin-waves localized on the lower density regions on the left and right sides of the trap. (See Fig. 4.)

III. III. QUADRUPOLE MODES

Experiments have investigated only the quadrupole modes. The increase in theoretical complication is considerable, especially when we include unequal scattering lengths. For the moments calculation we consider a function of the form

$$\delta m_p = (a_0 + a_1 \tilde{z}^2 + a_2 \tilde{z} \tilde{p}_z + a_3 \tilde{p}_z^2) m_p^{(0)}$$

for both longitudinal and transverse cases.

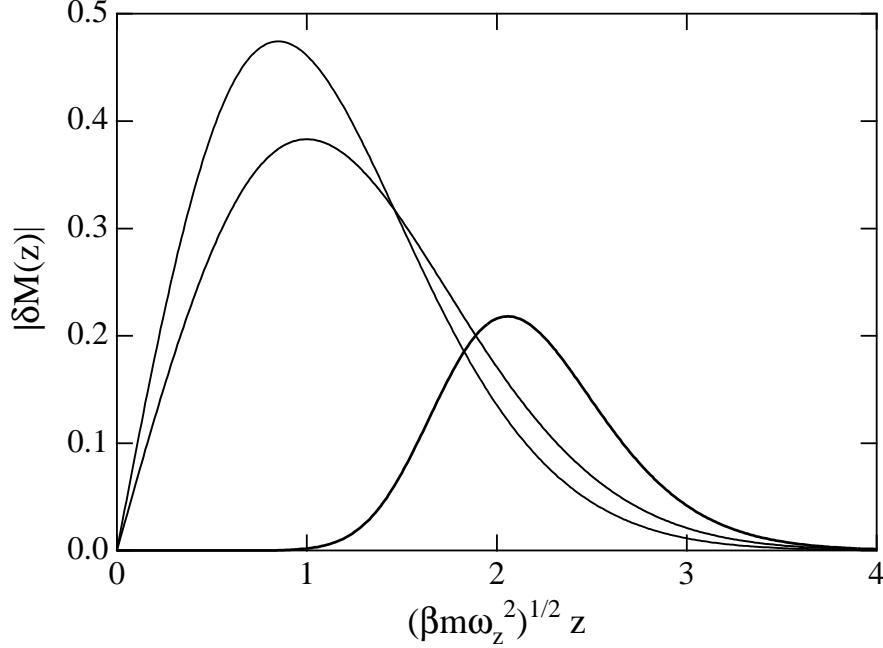


FIG. 4: Profiles $|\delta M(z)|$ of the the dipole modes vs. $\sqrt{\beta m \omega_z^2} z$, normalized with a Hermite weighting function. Tallest peak is the hydrodynamic mode for $\gamma_T = 0$ and $\tau_\perp = 0.01$. Middle peak is the moments method ansatz. Smallest peak is the hydrodynamic mode for $\gamma_T = 0.02\gamma_\perp$ and $\omega_z\tau = 0.01$.

A. a. Longitudinal quadrupole.

The equations we find are as follows:

$$a_0 = -(a_1 + a_3) \quad (28)$$

$$i\omega a_1 - \omega_z a_2 = 0 \quad (29)$$

$$2\omega_z a_1 + \left(i\omega + \frac{\gamma_\parallel}{2}\right) a_2 - 2\omega_z a_3 = 0 \quad (30)$$

$$\omega_z a_2 + (i\omega + \gamma_3) a_3 = 0 \quad (31)$$

where

$$\gamma_3 = \gamma_\parallel \left[1 + \frac{2}{5}(1 + \eta) \sum_\sigma \frac{t_{\sigma\sigma}^2}{t_{12}^2} f_\sigma \right]$$

When all the t 's are equal we have $\gamma_3 \rightarrow 9\gamma_\parallel/5$ for bosons and these equations reduce to those of Ref. [5].

We can again consider the solutions to the equations in limiting situations. For very large

$\omega_z \tau_{\parallel}$ (with $\tau_{\parallel} = 1/\gamma_{\parallel}$) we find the the three solutions

$$\omega \cong \begin{cases} \pm 2\omega_z + \frac{i}{4}(\gamma_3 + \gamma_{\parallel}) \\ i\frac{\gamma_3}{2} \end{cases} \quad (32)$$

In the small $\omega_z \tau_{\parallel}$ limit we again find a diffusive mode (proportional to a second order Hermite function in z^2) :

$$\omega = 4i\omega_z^2 \tau_{\parallel},$$

as well as two higher frequency decaying modes (one in zp_z and the other the Hermite in p^2) :

$$\omega \cong \begin{cases} \frac{i}{2\tau_{\parallel}} \\ i\gamma_3 \end{cases}. \quad (33)$$

Fig. 5 gives shows the modes for all $\omega_z \tau_{\parallel}$.

B. b. Transverse quadrupole

Taking moments of the quadrupole magnetic equation Eq. (6) and again going into the frame rotating at ω_0 gives the following equations

$$i\omega (a_0 + a_1 + a_3) - i\omega_{\parallel} a_1 + \gamma_T \left(a_0 + \frac{1}{2}a_1 + \frac{7}{6}a_3 \right) = 0 \quad (34)$$

$$i\omega (a_0 + 3a_1 + a_3) - i\omega_{\parallel} (a_0 + 6a_2) - 2\omega_z a_2 + \frac{\gamma_T}{2} \left(a_0 + \frac{3}{2}a_1 + \frac{7}{6}a_2 \right) = 0 \quad (35)$$

$$i \left(\omega - \frac{\omega_M}{2} \right) a_2 - i\omega_{\parallel} a_2 + \omega_z (a_1 - a_3) + \frac{\zeta_2}{2} a_2 = 0 \quad (36)$$

$$i\omega (a_0 + a_1 + 3a_3) - i\omega_{\parallel} a_1 + 2\omega_z a_2 - 2i\omega_M a_3 + \frac{7}{6}\gamma_T \left(a_0 + \frac{1}{2}a_1 \right) + \zeta_3 a_3 = 0 \quad (37)$$

where

$$\zeta_2 = \frac{4}{3}\gamma_0 \left\{ 1 + \frac{(1+\eta)}{8} \sum_{\sigma} f_{\sigma} \left[\left(\frac{t_{\sigma\sigma} - t_{12}}{t_{12}} \right)^2 + 6t_{\sigma\sigma} \frac{t_{\sigma\sigma} - t_{12}}{t_{12}^2} \right] \right\} \quad (38)$$

$$\zeta_3 = \gamma_0 \left[\frac{8}{3} + (1+\eta) \frac{77}{60} + \frac{(1+\eta)}{t_{12}^2} \sum_{\sigma} f_{\sigma} \left(\frac{79}{20} t_{\sigma\sigma}^2 - \frac{25}{6} t_{\sigma\sigma} t_{12} \right) \right] \quad (39)$$

In the case of equal values of all the t 's we have $\zeta_2 \rightarrow \gamma_{\parallel}$ and $\zeta_3 \rightarrow 18\gamma_{\parallel}/5$ for bosons. As in the dipole case the first equation represents a nonconserved monopole mode. If we take ω_{\parallel} and γ_T to zero, this equation represents the zero frequency monopole mode. We see then that a non-zero ω_{\parallel} couples the monopole and quadrupole modes, because it arises from a quadratic external field. We will now consider solutions in various special cases.

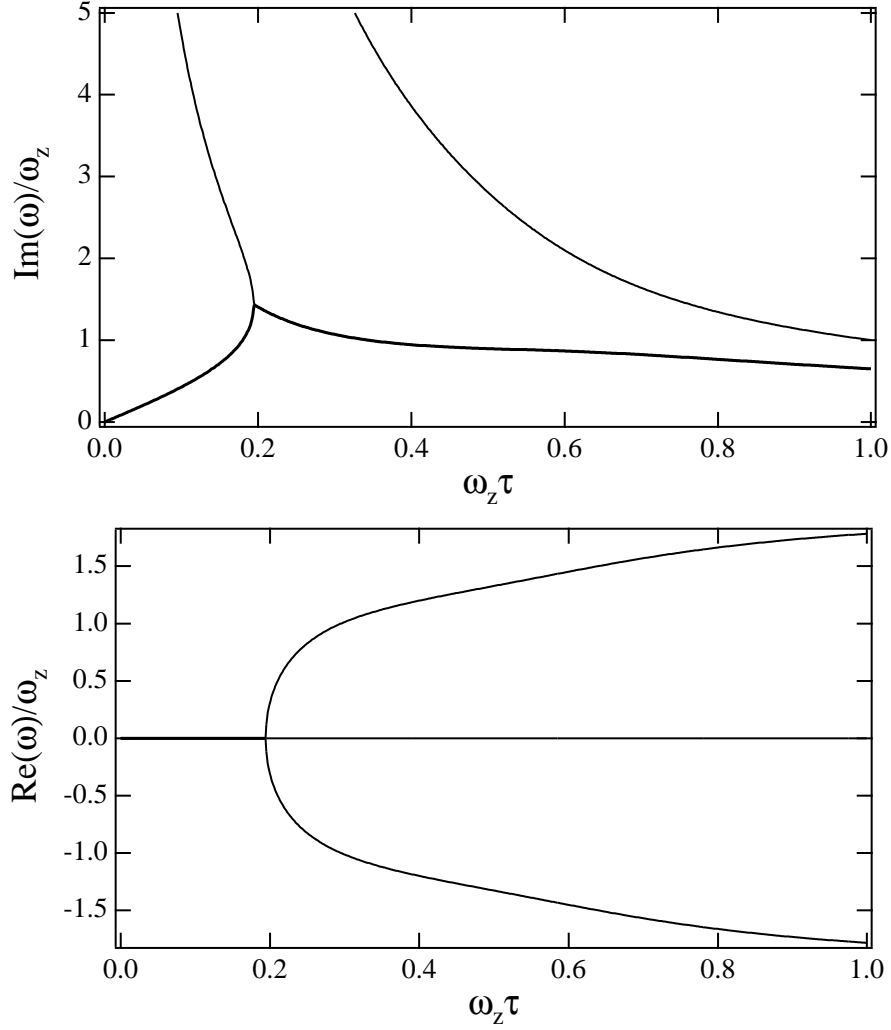


FIG. 5: Imaginary(top) and real (bottom) components of longitudinal quadrupole spin wave modes versus average relaxation time τ_{\parallel} . The diffusive mode is shown with darker lines.

Zero values of γ_T , ω_M , and ω_{\parallel} : When all three of these parameters are set to zero, we get modes that look just exactly like the longitudinal case of Fig. 5. The diffusive mode's imaginary part goes to zero with $\omega_z \tau_2$ as expected; here $\tau_2 = 1/\zeta_2$. Two of the modes have degenerate relaxation times.

Non-zero ω_M ; zero γ_T and ω_{\parallel} : With non-zero mean-field value ω_M the degeneracy is now split as shown in Fig. 6. For small $\omega_z \tau_2$, the real parts of two of the modes have finite values, ω_M and $\omega_M/2$, but the imaginary parts of those modes still diverge so that they are very short-lived. The diffusive mode, whose imaginary and real parts both go to zero as $\tau_2 \rightarrow 0$,

is given, to order $(\omega_z \tau_2)^2$, by

$$\omega \cong 4\omega_z^2 \tau_2 (i - \omega_M \tau_2) \quad (40)$$

This behavior is of the same form as the transverse dipole mode, Eq.(21) with the factor of 4 occurring for this higher order mode. The relaxation time τ_2 reduces to τ_{\parallel} only when all the t 's are equal or for fermions. So even ignoring the effect of γ_T we would have boson diffusive anisotropy since τ_2 is not the same as τ_{\parallel} . The monopole mode decay rate vanishes in this case.

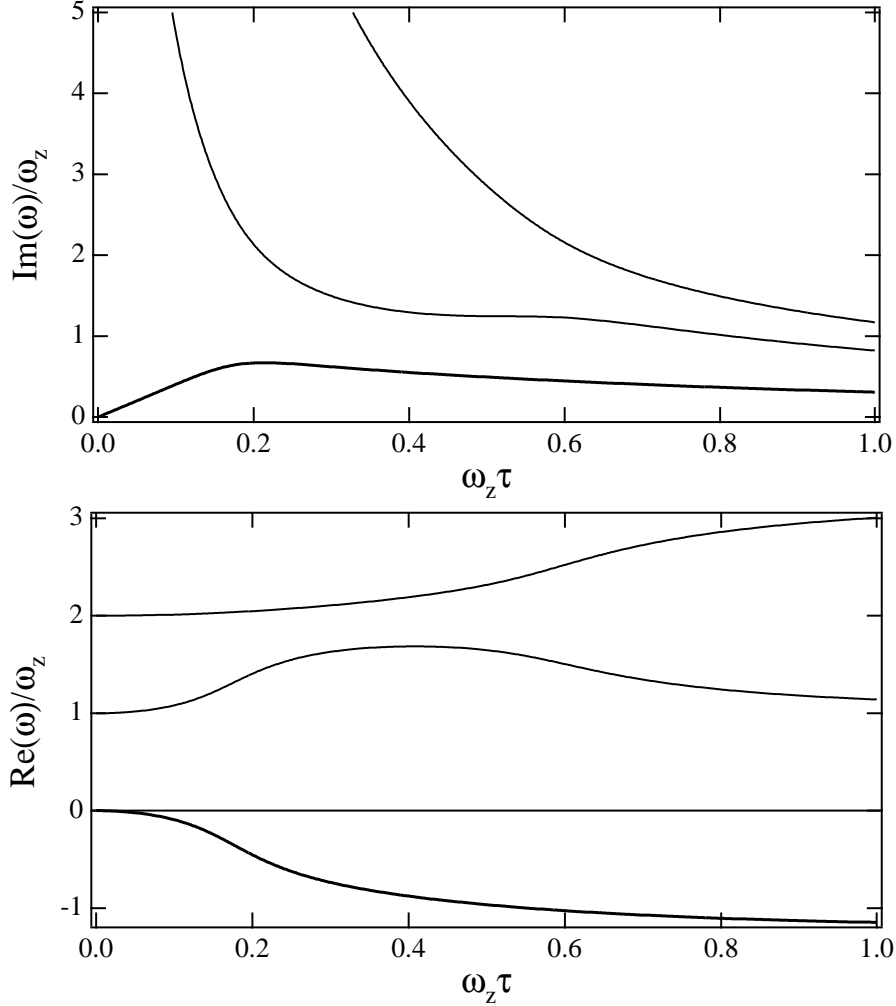


FIG. 6: Imaginary(top) and real (bottom) components of longitudinal quadrupole spin wave modes versus average relaxation time τ_2 with $\omega_M = 2\omega_z$, $\gamma_T = 0$, $\omega_{\parallel} = 0$. The degeneracy in some imaginary parts is lifted, and the diffusive mode (dark lines) now has a real part.

Non-zero γ_T ; and zero ω_{\parallel} : As in the dipolar case the existence of the non-conservation

terms means a different behavior for small τ_2 as we now see in Fig. 7. From the moments calculation we find again that the imaginary parts of *all* modes, including both monopole and diffusive, now diverge proportional to $\gamma_T \sim 1/\tau_2$. The figure shows just the imaginary parts of the monopole and diffusive, indicating that the transverse magnetization is no longer conserved for bosons. However, as in the dipole case, a more accurate analysis shows that the small τ behavior shows a divergence as $\sqrt{\log(1/\omega_z\tau_2)}$. Fermions on the other hand behave as usual, because their scattering can depend only on t_{12} and not on the difference in t values.

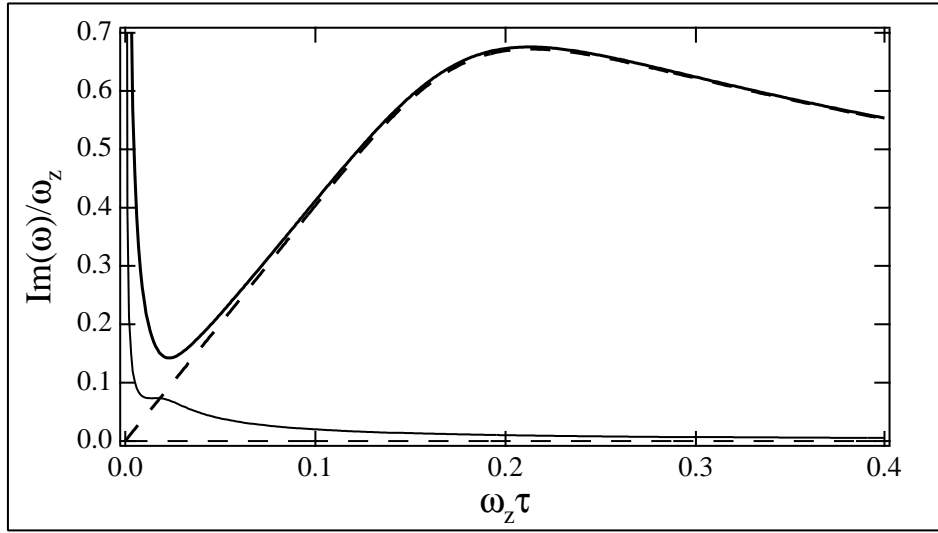


FIG. 7: Imaginary components of transverse monopole and quadrupole boson spin wave modes versus average relaxation time τ_2 with $\gamma_T = 0.002/\tau_2$ and $\omega_{\parallel} = 0$. The solid lines are the modes with γ_T non-zero and the dashed lines show the previous results with γ_T zero. Now these modes diverge at small τ .

Non-zero ω_{\parallel} ; zero ω_M and γ_T : The quantity ω_{\parallel} arises from the existence of an external quadratic potential difference between the two species. Because it is quadratic, it causes a coupling between the monopole and quadrupole modes. In Fig. 8 we show the transverse quadrupole modes with a small value of $\omega_{\parallel} > 0$. We see that it does cause splitting between the previously degenerate relaxation times. Further, the real frequencies that vanished for small $\omega_z\tau_2$ now are now finite and split with non-trivial structure. A particularly interesting feature for quite small $\omega_z\tau_2$ is the near coalescing of the imaginary monopole and diffusive modes due to the quadratic coupling. The upper mixed mode mode, instead of going to zero

as $4\omega_z\tau_2$, as it did when diffusive now has half that slope as demonstrated in Fig. 9 .

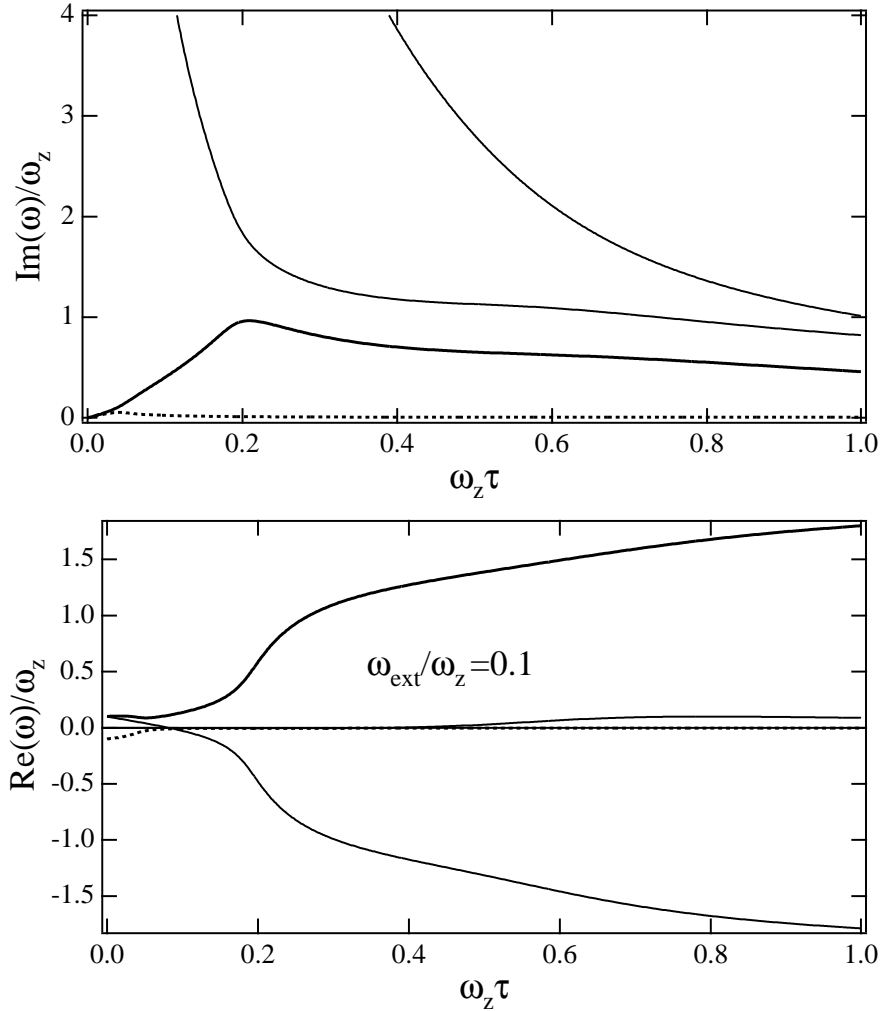


FIG. 8: Imaginary (top) and real (bottom) components of the transverse monopole and quadrupole boson spin wave modes versus average relaxation time τ_2 with $\omega_{\parallel} = 0.1\omega_z$. The darker lines are the diffusive modes and the dotted line is the monopole mode; these are now mixed at small τ_2 . The very small τ_2 behavior of the diffusive relaxation frequency and all the real modes is altered by the presence of this coupling with the monopole mode. See the next figure.

IV. IV. DISCUSSION

We have shown that rather unusual differences between Bose and Fermi gases in the Boltzmann limit can arise in spin-diffusion experiments, when the scattering lengths for dif-

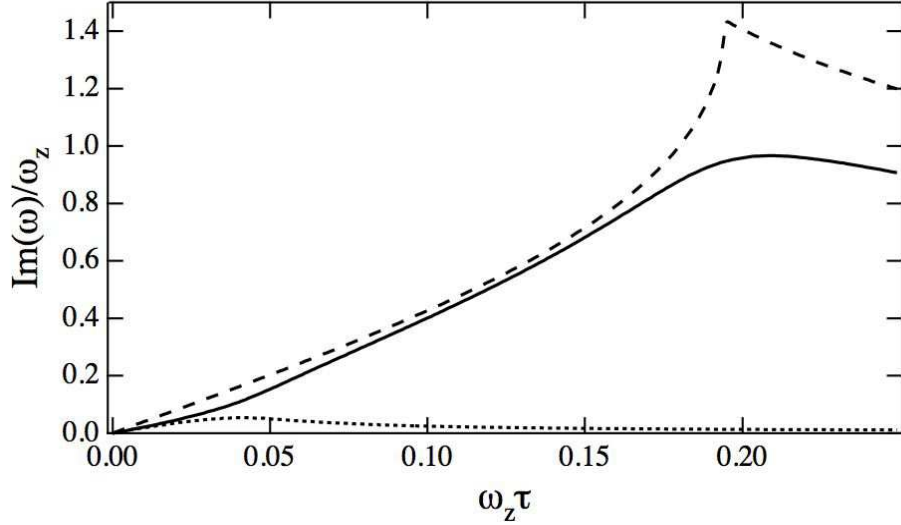


FIG. 9: Imaginary components of the transverse monopole (dotted line) and diffusive quadrupole (solid line) boson spin wave modes versus average relaxation time τ_2 with $\omega_{\parallel} = 0.1\omega_z$. The dashed lines shows the $\omega_{\parallel} = 0$ case for comparison.

ferent spin configurations are not the same, and when the effective field for the transverse modes does not vanish. For fermions there is no distinction between longitudinal and transverse modes. In the fermion case to see such an anisotropy one would have to go to the degenerate limit where phase space differences would lead to a difference between longitudinal and transverse modes.[10] However, for bosons, longitudinal and transverse modes show striking differences when the scattering lengths are not the same. Indeed in the transverse case the magnetization is no longer conserved as it is in the longitudinal case; instead of a linear $\omega_z \tau$ dependence of the spin diffusive mode one finds a divergence.

In experiments on Rb, the interaction anisotropy is very small. To test the novel effects predicted here one might use Na,[18] which has a difference in interaction parameters; Numerically we estimate that for ^{23}Na γ_{\perp} can differ from γ_{\parallel} by as much as 14% with $\gamma_T/\gamma_{\perp} \approx 0.04$. Interaction differences might also be induced by using Feshbach resonance methods.

We thank Dr. Jean-Noël Fuchs and Prof. David Hall for useful discussions.

-
- [1] H. J. Lewandowski, D. M. Harber, D. L. Whitaker, and E. A. Cornell, Phys. Rev. Lett. **88**, 070403 (2002).

- [2] J. M. McGuirk, H. L. Lewandowski, D. M. Harper, T. Nikuni, J. E. Williams, and E. A. Cornell, Phys. Rev. Lett. **89**, 090402 (2002).
- [3] M. O. Oktel and L. S. Levitov, Phys. Rev. Lett. **88**, 230403 (2002).
- [4] J. N. Fuchs, D. M. Gangardt, and F. Laloë, Phys. Rev. Lett. **88**, 230404 (2002); Eur. Phys. J. D **25**, 57 (2003).
- [5] J. E. Williams, T. Nikuni, and C. W. Clark, Phys. Rev. Lett. **88**, 230405 (2002); T. Nikuni, J. E. Williams, and C. W. Clark, Phys. Rev. A **66**, 043411 (2002).
- [6] J. N. Fuchs, O. Prévoté, and D. M. Gangardt, Eur. Phys. J. D **25**, 161 (2003).
- [7] T. Nikuni and J. E. Williams, J. Low Temp. Phys. **133**, 323 (2003).
- [8] A. S. Bradley and C. W. Gardiner, J. Phys. B: At. Mol. Opt. Phys. **35**, 4299 (2002).
- [9] H. Akimoto, D. Candela, J. S. Xia, W. J. Mullin, E. D. Adams, and N. S. Sullivan, Phys. Rev. Lett. **90**, 105301 (2003). This paper has a rather complete list of theoretical and experimental references for homogeneous real-spin Fermi fluids.
- [10] W. J. Mullin and J. W. Jeon, Jour. Low Temp. Phys., **88**, 433 (1992).
- [11] J. Jeon and H. R. Glyde, Phys. Rev. B **43**, 5338 (1991).
- [12] I. A. Fomin, JETP Lett. **65**, 749 (1997).
- [13] V. P. Mineev, *Phys. Rev. B* **69**, 1444 (2004); cond-mat/0404539; cond-mat/0411361.
- [14] W. J. Mullin and R. J. Ragan, *Jour. Low Temp. Phys.*, **138**, 73 (2005)
- [15] W. J. Mullin and R. J. Ragan, *Jour. Low Temp. Phys.*, **138**, 711 (2005)
- [16] We consider temperatures such that the distribution function is Boltzmann, but the pair interactions are quantum mechanical with s-wave scattering predominating. This can occur if the interparticle spacing is much greater than the de Broglie wavelength which, in turn, is much greater than the scattering length.
- [17] C. Lhuillier and F. Laloe, J. Phys. (Paris) **43**, 197 (1982); **43**, 225 (1982).
- [18] A. Görlitz, T. L. Gustavson, A. E. Leanhardt, R. Low, A. P. Chikkatur, S. Gupta, S. Inouye, D. E. Pritchard, and W. Ketterle, Phys. Rev. Lett. **90**, 090401 (2003).